Editors' Suggestion

First observation of the $B^+ \to D_s^+ D_s^- K^+$ decay

R. Aaij *et al.*[*]

(LHCb Collaboration)

The $B^+ \to D_s^+ D_s^- K^+$ decay is observed for the first time using proton-proton collision data collected by the LHCb detector at center-of-mass energies of 7, 8, and 13 TeV, corresponding to an integrated luminosity of 9 fb^{-1}. Its branching fraction relative to that of the $B^+ \to D^+ D^- K^+$ decay is measured to be $\frac{\mathcal{B}(B^+ \to D_s^+ D_s^- K^+)}{\mathcal{B}(B^+ \to D^+ D^- K^+)} = 0.525 \pm 0.033 \pm 0.027 \pm 0.034$, where the first uncertainty is statistical, the second systematic, and the third is due to the uncertainties on the branching fractions of the $D_s^\pm \to K^\mp K^\pm \pi^\pm$ and $D^\pm \to K^\mp \pi^\pm \pi^\pm$ decays. This measurement fills an experimental gap in the knowledge of the family of Cabibbo-favored $\bar{b} \to \bar{c} c \bar{s}$ transitions and opens the path for unique studies of spectroscopy in future.

I. INTRODUCTION

The family of $B \to D_{(s)}^{(*)} \bar{D}_{(s)}^{(*)} K^{(*)}$ decays proceeds at the quark level via the Cabibbo-favored $\bar{b} \to \bar{c} c \bar{s}$ transition.[1] Such decays provide an excellent laboratory for investigations of open- and hidden-charm meson spectroscopy [1–7], covering both conventional and exotic states. Additionally, measurements of the amplitude structures in the $D_{(s)}^{(*)} \bar{D}_{(s)}^{(*)}$ system of these decays can offer important information to the theoretical calculations of the charm-loop contributions to $b \to s\ell^+\ell^-$ processes that are sensitive to physics beyond the Standard Model [8].

There have already been experimental studies of $B \to D^{(*)} \bar{D}^{(*)} K^{(*)}$ decays by the ALEPH, *BABAR*, Belle, and LHCb collaborations [1–7,9–13], not only making observations of some of these decay channels but also leading to discoveries of new resonances. However, all such measurements to date focus only on B decays with a $D^{(*)} \bar{D}^{(*)}$ pair in the final state. Decays involving the $D_s^{(*)+} D_s^{(*)-}$ pair, e.g. $B^+ \to D_s^+ D_s^- K^+$, have never been explored. The $D_s^+ D_s^-$ system is attractive as it provides a unique insight into the charmonium(like) spectroscopy. Conventional charmonium mesons with natural spin (J), parity (P), and charge-parity (C) quantum numbers ($J^{PC} = 0^{++}, 1^{--}, 2^{++}, \ldots$), e.g. $\psi(4040)$ [14],

are expected to predominantly decay into the $D^{(*)} \bar{D}^{(*)}$ final state. In contrast, charmoniumlike hadrons with the $c\bar{c}s\bar{s}$ constituents could have a larger partial decay width to the $D_s^+ D_s^-$ final state than that to $D^{(*)} \bar{D}^{(*)}$. A few candidates for $c\bar{c}s\bar{s}$ states have been observed in the $J/\psi\phi$ final state from $B^+ \to J/\psi\phi K^+$ decays [15]. They might also decay into $D_s^+ D_s^-$ and contribute to the $B^+ \to D_s^+ D_s^- K^+$ decay.
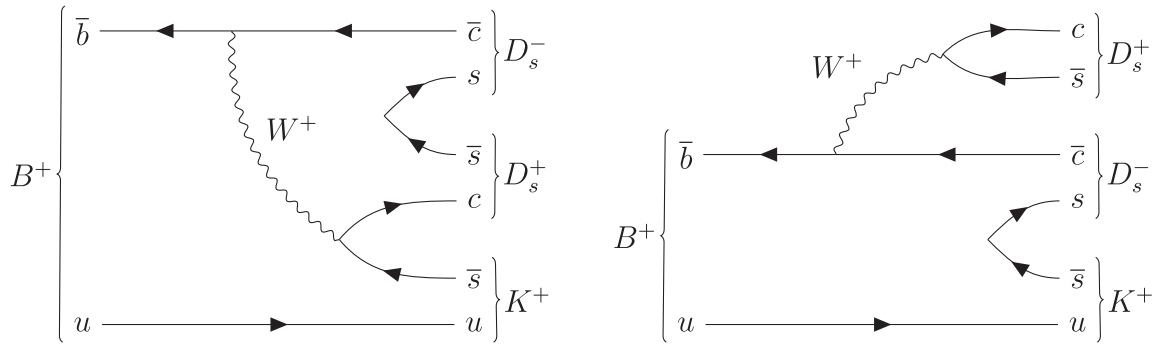
This paper presents the first observation of the $B^+ \to D_s^+ D_s^- K^+$ decay. The contributing tree-level Feynman diagrams of this decay are shown in Fig. 1. The branching fraction of the $B^+ \to D_s^+ D_s^- K^+$ decay is measured relative to that of the normalization channel $B^+ \to D^+ D^- K^+$. The two channels have a similar decay topology, so the corresponding systematic uncertainties on the branching-fraction ratio are expected to largely cancel. The measurement uses the proton-proton (pp) collision data collected by the LHCb experiment in 2011, 2012, and 2015–2018 at center-of-mass energies of 7, 8, and 13 TeV, respectively, corresponding to a total integrated luminosity of 9 fb^{-1}. The branching fraction of the $B^+ \to D_s^+ D_s^- K^+$ decay is an essential input to obtain the partial width information of the near-threshold structure in the $D_s^+ D_s^-$ system analyzed in the accompanying paper [16].

II. DETECTOR AND SIMULATION

The LHCb detector [17,18] is a single-arm forward spectrometer covering the pseudorapidity range $2 < \eta < 5$, designed for the study of particles containing b or c quarks. The detector includes a high-precision tracking system consisting of a silicon-strip vertex detector surrounding the pp interaction region [19], a large-area silicon-strip detector located upstream of a dipole magnet with a bending power of about 4 Tm, and three stations of

---

FIG. 1.   Feynman diagrams contributing to the $B^+ \to D_s^+ D_s^- K^+$ decay.

silicon-strip detectors and straw drift tubes [20,21] placed downstream of the magnet. The tracking system provides a measurement of the momentum, p, of charged particles with a relative uncertainty that varies from 0.5% at low momentum to 1.0% at 200 GeV. The minimum distance of a track to a primary pp collision vertex (PV), the impact parameter, is measured with a resolution of $(15 + 29/p_T)$ μm, where p_T is the component of the momentum transverse to the beam, in GeV. Different types of charged hadrons are distinguished using information from two ring-imaging Cherenkov detectors [22]. Photons, electrons, and hadrons are identified by a calorimeter system consisting of scintillating-pad and preshower detectors, an electromagnetic and a hadronic calorimeter. Muons are identified by a system composed of alternating layers of iron and multiwire proportional chambers [23].

The online event selection is performed by a trigger [24], which consists of a hardware stage, based on information from the calorimeter and muon systems, followed by a software stage, which applies a full event reconstruction. At the hardware trigger stage, events are required to have a muon with high p_T or a hadron, photon, or electron with high transverse energy in the calorimeters. The hadron can originate from either the studied decay or the rest of the event. The software trigger requires a two-, three-, or four-track secondary vertex with a significant displacement from any PV. At least one charged particle must have a transverse momentum $p_T > 1.6$ GeV and be inconsistent with originating from a PV. A multivariate algorithm [25,26] is used for the identification of secondary vertices consistent with the decay of a b hadron.

Simulation is required to model the effects of the detector acceptance and the imposed selection requirements for the $B^+ \to D_s^+ D_s^- K^+$ and $B^+ \to D^+ D^- K^+$ decays. In the simulation, pp collisions are generated using PYTHIA [27] with a specific LHCb configuration [28]. Decays of unstable particles are described by EvtGen [29], in which final-state radiation is generated using PHOTOS [30]. The interaction of the generated particles with the detector, and its response, are implemented using the GEANT4 toolkit [31] as described in Ref. [32]. The underlying pp interaction is

reused multiple times, with an independently generated signal decay for each event [33]. The particle-identification (PID) response is not well described in the LHCb simulation, and is corrected to match that in data. The correction is determined from calibration samples using a reweighing approach, the so-called PID transformation [34,35].

III. EVENT SELECTION

The $B^+ \to D_s^+ D_s^- K^+$ and $B^+ \to D^+ D^- K^+$ decays are reconstructed using the $D_s^+ \to K^+ K^- \pi^+$ and $D^+ \to K^- \pi^+ \pi^+$ decay channels, respectively. The selection starts by choosing well-reconstructed tracks that are inconsistent with originating from any PV. The selected tracks should have PID information consistent with the corresponding final-state kaons and pions. Additionally, the opening angle between any two final-state charged tracks must be larger than 0.5 mrad to reduce potential reuse of track segments. The D^+ and D_s^+ candidates, obtained by combining K and π candidates, are required to have good-quality vertices and their reconstructed masses must lie within ± 25 MeV of the known masses [14], corresponding to about three times the mass resolution. The B^+ candidates are then formed by combining $D_{(s)}^+$, $D_{(s)}^-$, and K^+ candidates. The B^+ decay vertex must be well reconstructed and significantly displaced from all PVs. The B^+ candidate is required to have a flight direction pointing back to the PV where it is produced, referred to hereafter as the associated PV. To reduce the contamination from the non-double-charm (NDC) B^+ decay candidates that have the same set of the final-state tracks as that of the $B^+ \to D_{(s)}^+ D_{(s)}^- K^+$ decay but do not involve two real $D_{(s)}^\pm$ mesons, requirements on the distances between the B^+ and $D_{(s)}^\pm$ vertices are imposed, taking advantage of the nonzero flight distance of the $D_{(s)}^\pm$ meson. A kinematic fit [36] is employed to improve the B^+ mass resolution by constraining the $D_{(s)}^\pm$ mass to its known value [14] and requiring the B^+ candidate to originate from the associated PV. A second kinematic fit with an additional B^+ mass constraint is utilized when
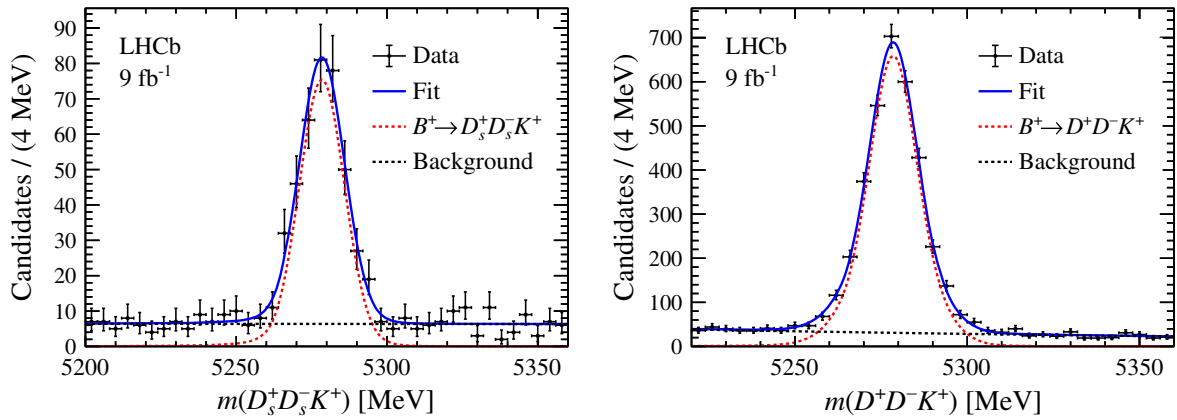
FIG. 2. Invariant-mass distributions of reconstructed (left) $D_s^+ D_s^- K^+$ and (right) $D^+ D^- K^+$ candidates. The fit results are overlaid.

investigating the distributions of the Dalitz-plot variables in $B^+ \to D_s^+ D_s^- K^+$ and $B^+ \to D^+ D^- K^+$ decays.

Gradient boosted decision tree (BDTG) [37–39] classifiers are employed to reduce further background from random combinations of tracks, referred to hereafter as combinatorial background. The classifier is trained separately for the $B^+ \to D_s^+ D_s^- K^+$ and $B^+ \to D^+ D^- K^+$ channels using the corresponding simulated sample as the signal proxy and candidates in data with a reconstructed B^+ mass of 5360–6000 MeV as the background proxy. The discriminating variables used in the classifier include PID information of the final-state tracks, kinematic properties, and the decay topology of the B^+ and $D_{(s)}^\pm$ candidates. The selection criterion for the response of each classifier is optimized by maximizing the figure of merit, $N_S / \sqrt{N_S + N_B}$, separately for each channel. Here, N_S (N_B) is the expected signal (background) yield within ± 20 MeV of the known B^+ mass [14], estimated as the product of the signal (background) yield without any BDTG requirement and the signal efficiency (1-background-rejection factor) for a given criterion. The signal and background yields without the BDTG requirements in each channel are evaluated using a simple fit to the reconstructed B^+ mass distribution with the signal and background probability density functions (PDFs) modeled by a Gaussian function and an exponential function, respectively. The signal efficiency and background-rejection factor are directly obtained from the samples used to test the classifiers.

Multiple candidates, found in a few percent of pp collision events, are mostly due to the duplicated use of tracks from the same event. In each event, the candidate having the smallest χ^2 of the kinematic fit without the B^+ mass constraint is retained.

The reconstructed $D_s^+ D_s^- K^+$ and $D^+ D^- K^+$ invariant-mass distributions after all the selection requirements are shown in Fig. 2. The mass windows, $(5280 - 80, 5280 + 80)$ MeV and $(5280 - 60, 5280 + 80)$ MeV, for the signal and normalization channels, respectively, are chosen to

exclude the contributions of partially reconstructed background with a missing photon from $D_s^{*\pm} \to D_s^\pm \gamma$ or $D^{*\pm} \to D^\pm \gamma$ decay. Here, the tighter lower-side threshold for the $B^+ \to D^+ D^- K^+$ channel than that for the $B^+ \to D_s^+ D_s^- K^+$ channel is found necessary to exclude all visible tails of the partially reconstructed background [5,6]. These mass windows are also sufficient to exclude partially reconstructed background with a missing π^0 meson from $D_s^{*+} \to D_s^+ \pi^0$ or $D^{*+} \to D^+ \pi^0$ decay, as the reconstructed $D_s^+ D_s^- K^+$ or $D^+ D^- K^+$ mass is shifted at least 135 MeV below the B^+ mass peak [14]. For both the $B^+ \to D_s^+ D_s^- K^+$ signal and $B^+ \to D^+ D^- K^+$ normalization channels, any potential background resulting from the misidentification of a single K or π would originate from Cabbibo-suppressed decays and thus is negligible.

IV. SIGNAL EXTRACTION

Unbinned extended maximum-likelihood fits to the mass distributions of the B^+ candidates are performed to determine the signal yields in the $B^+ \to D_s^+ D_s^- K^+$ and $B^+ \to D^+ D^- K^+$ channels. The signal PDF is a sum of two crystal ball (CB) functions [40] with a common peak position and opposite-side tails. The tail parameters are fixed to the values obtained from the simulated $B^+ \to D^+ D^- K^+$ or $B^+ \to D_s^+ D_s^- K^+$ sample and the fractions of the two CB functions are set to 0.5. All other parameters including the peak position, the widths of the two CB functions are free to vary in the fit to data. The combinatorial background is modeled using an exponential function with its parameter free to vary in the fit.

The fit results are shown in Fig. 2. A signal yield of $N_{\text{sig}} = 360 \pm 22$, where the uncertainty is statistical only, is obtained for the $B^+ \to D_s^+ D_s^- K^+$ decay, with a purity in a ± 20 MeV window around the peak of approximately 84%. The statistical significance of the $B^+ \to D_s^+ D_s^- K^+$ decay is evaluated under the assumption that the log-likelihood difference between the fit without the signal component and the default fit follows a χ^2 distribution with the number
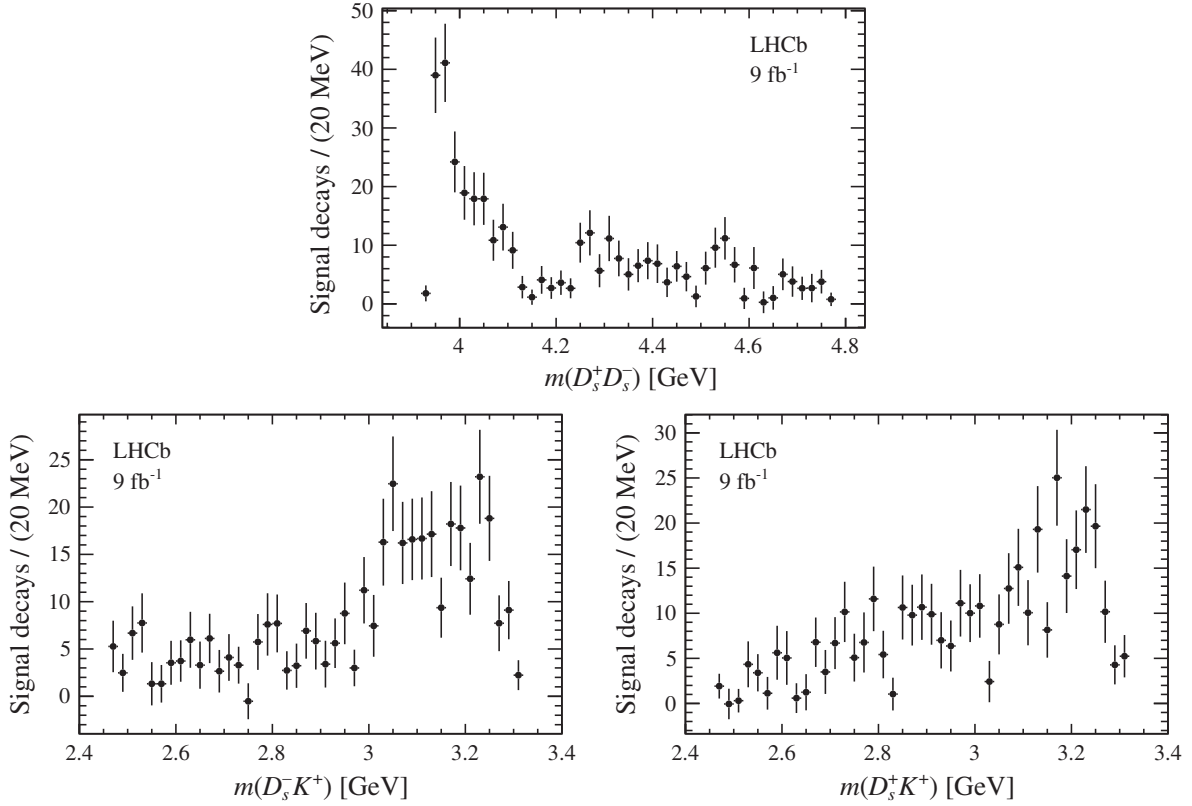
FIG. 3. Distributions of background-subtracted invariant mass of the (top) $D_s^+ D_s^-$, (bottom left) $D_s^- K^+$, and (bottom right) $D_s^+ K^+$ systems of the $B^+ \rightarrow D_s^+ D_s^- K^+$ decay.

of degrees of freedom being the difference in the number of free parameters of the two fits [41]. Given the log-likelihood difference of 646 with four degrees of freedom, the significance is found to be much larger than 10 standard deviations (σ). Since the systematic uncertainty discussed in Sec. VI is not expected to greatly reduce the significance, this result constitutes the first observation of the $B^+ \rightarrow D_s^+ D_s^- K^+$ decay. The signal yield in the $B^+ \rightarrow D^+ D^- K^+$ channel is obtained as $N_{\rm norm} = 3215 \pm 65$, where the uncertainty is statistical, and the purity is around 91% using the same mass window definition. The $B^+ \rightarrow D^+ D^- K^+$ signal yield is larger and the corresponding purity is lower compared with those in Refs. [5,6], reflecting that looser selection criteria are imposed in this paper.

To demonstrate the potential contributions from intermediate resonances in the $B^+ \rightarrow D_s^+ D_s^- K^+$ decay, the invariant-mass distributions of the $D_s^+ D_s^-$, $D_s^- K^+$, and $D_s^+ K^+$ combinations, denoted, respectively, as $m(D_s^+ D_s^-)$, $m(D_s^- K^+)$, and $m(D_s^+ K^+)$, are shown in Fig. 3. The combinatorial background is subtracted using the *sPlot* method [42] with the B^+ candidate mass exploited as the discriminating variable. A clear peaking structure is seen at the $D_s^+ D_s^-$ mass threshold, corresponding to a charmonium (like) candidate. An amplitude analysis is performed to study the resonant contributions in the $B^+ \rightarrow D_s^+ D_s^- K^+$

decay, presented separately in Ref. [16]. The intermediate resonant contributions to the $B^+ \rightarrow D^+ D^- K^+$ decay have been studied in the previous LHCb analyses described in Refs. [5,6].

Pseudoexperiments are carried out to check potential biases on the extracted signal yields in the signal and normalization channels. Numerous samples are randomly generated according to the determined PDFs where the number of signal (background) candidates in each sample is varied according to a Poissonian distribution with the mean set to the determined signal (background) yield, referred to as the default result. The signal yield in each generated sample is determined by a fit to the B^+ candidate mass distribution and its variation from the default result is quantified as the pull value, $(N_i - N_0)/\sigma_i$, where N_i and σ_i are the signal yield and its statistical uncertainty in the ith sample, respectively, and N_0 is the default signal yield. The pull distribution is then fitted using a Gaussian function. The mean represents the bias on the signal yield relative to the size of its statistical uncertainty. The bias is $\delta_{\rm sig} = 0.09 \pm 0.01$ for the signal channel and is corrected for in the branching fraction calculation. Here, the uncertainty is due to limited number of the pseudoexperiments. No obvious bias is found on the signal yield for the normalization channel.

The measured $B^+ \rightarrow D_s^+ D_s^- K^+$ and $B^+ \rightarrow D^+ D^- K^+$ signal yields contain residual NDC contributions, which
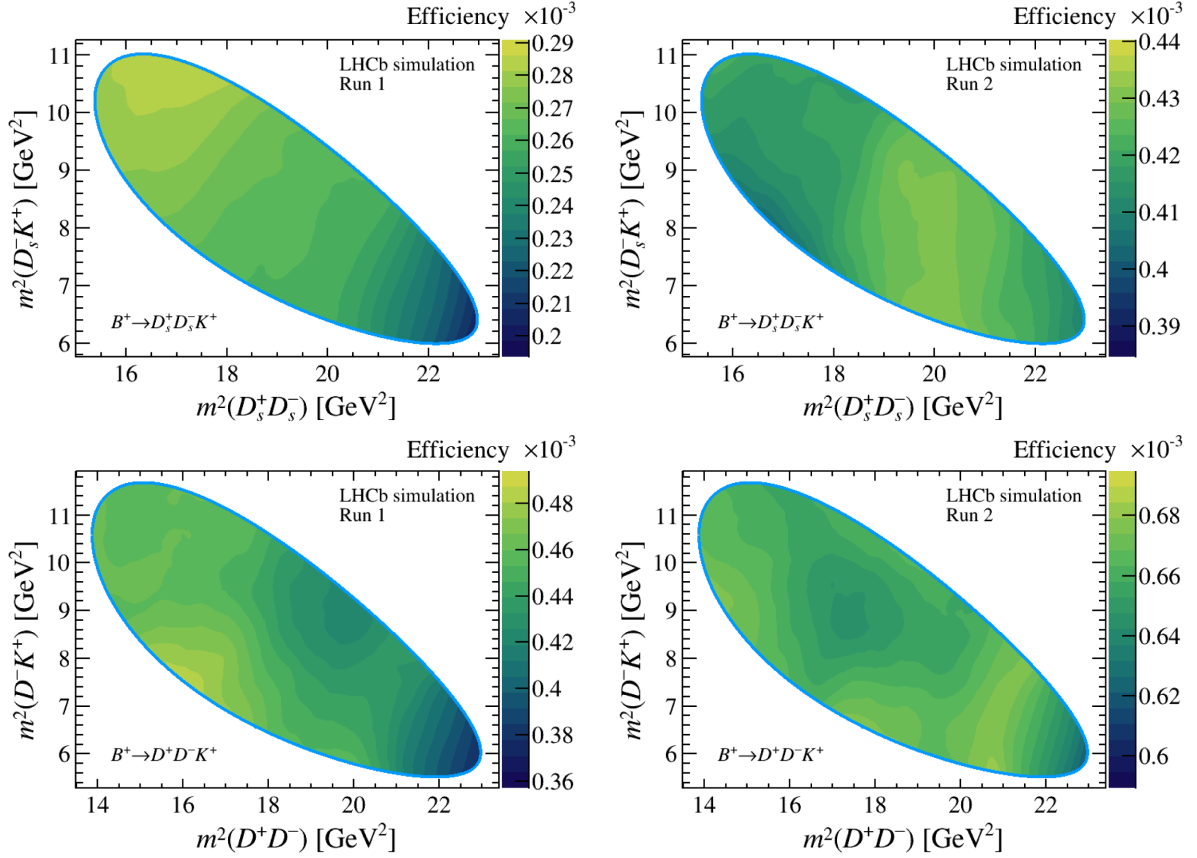
FIG. 4. Efficiency as a function of the Dalitz-plot variables for the (top) $B^+ \to D_s^+ D_s^- K^+$ and (bottom) $B^+ \to D^+ D^- K^+$ decays, calculated separately for the (left) run 1 and (right) run 2 periods.

need to be subtracted in the branching fraction calculation presented in Sec. V. The expected NDC yields are estimated using the same method as that in Refs. [5,6], based on the number of candidates in the $D_{(s)}^\pm$ mass sidebands, which are 30–80 MeV away from the known $D_{(s)}^\pm$ mass [14]. The fractions of the NDC yields in the total B^+ signal yields, are found to be $f_{\mathrm{NDC}}^{\mathrm{sig}} = (5.2 \pm 2.7)\%$ and $f_{\mathrm{NDC}}^{\mathrm{norm}} = (3.2 \pm 0.6)\%$ for the $B^+ \to D_s^+ D_s^- K^+$ and $B^+ \to D^+ D^- K^+$ channels, respectively. The uncertainties are due to the limited number of the candidates in the $D_{(s)}^\pm$ mass sidebands. The larger NDC-background contamination in the $B^+ \to D^+ D^- K^+$ channel compared with that in Refs. [5,6] is due to relatively looser selection requirements in this paper.

V. BRANCHING FRACTION CALCULATION

The branching fraction of the $B^+ \to D_s^+ D_s^- K^+$ decay is measured relative to that of the $B^+ \to D^+ D^- K^+$ decay,

$$\mathcal{R} \equiv \frac{\mathcal{B}(B^+ \to D_s^+ D_s^- K^+)}{\mathcal{B}(B^+ \to D^+ D^- K^+)} = \frac{N_{\mathrm{sig}}^{\mathrm{corr}}}{N_{\mathrm{norm}}^{\mathrm{corr}}} \left[\frac{\mathcal{B}(D^+ \to K^- \pi^+ \pi^+)}{\mathcal{B}(D_s^+ \to K^- K^+ \pi^+)} \right]^2, \quad (1)$$

where the branching fractions of the decays $B^+ \to D^+ D^- K^+$, $D^+ \to K^- \pi^+ \pi^+$, and $D_s^+ \to K^- K^+ \pi^+$ are taken from Refs. [11,14]. The efficiency-corrected signal yields of the $B^+ \to D_s^+ D_s^- K^+$ and $B^+ \to D^+ D^- K^+$ channels, $N_{\mathrm{sig}}^{\mathrm{corr}}$ and $N_{\mathrm{norm}}^{\mathrm{corr}}$, are determined as

$$N_{\mathrm{sig}}^{\mathrm{corr}} = \sum_i \frac{w_{\mathrm{sig},i}}{\epsilon_{\mathrm{sig},i}(m^2(D_s^+ D_s^-), m^2(D_s^- K^+))}, \quad (2)$$

$$N_{\mathrm{norm}}^{\mathrm{corr}} = \sum_i \frac{w_{\mathrm{norm},i}}{\epsilon_{\mathrm{norm},i}(m^2(D^+ D^-), m^2(D^- K^+))}, \quad (3)$$

where the index i runs over all the selected B^+ candidates in the signal or normalization channel. The weight $w_{\mathrm{sig},i}$ or $w_{\mathrm{norm},i}$ assigned to each candidate is obtained using the *sPlot* method [42]; summing over these weights effects a statistical subtraction of the combinatorial background contribution. The discriminating variable is the reconstructed $D_s^+ D_s^- K^+$ or $D^+ D^- K^+$ mass, as shown in Fig. 2. The efficiencies $\epsilon_{\mathrm{sig},i}$ and $\epsilon_{\mathrm{norm},i}$, determined using simulated samples, take into account the effects of geometric acceptance, reconstruction, and selection requirements. They are evaluated separately in the two data-taking

periods, 2011–2012 (run 1) and 2015–2018 (run 2), because of the differences in the collision energy and the detector configuration, and are shown in Fig. 4 as functions of the Dalitz-plot variables of the corresponding decays. The kernel density estimation (KDE) [43] technique is employed to obtain smooth efficiency distributions across the Dalitz plots. Finally, the efficiency-corrected yields are determined to be $N_{\mathrm{sig}}^{\mathrm{corr}} = (9.5 \pm 0.6) \times 10^5$ and $N_{\mathrm{norm}}^{\mathrm{corr}} = (5.33 \pm 0.11) \times 10^6$, where the uncertainties are statistical only.

Before obtaining the branching-fraction ratio $\mathcal{R}$, it is necessary to subtract the NDC background contributions and to correct for the small fit bias on the extracted signal yield in the $B^+ \to D_s^+ D_s^- K^+$ channel. These two effects are accounted for by introducing in Eq. (1) two correction factors: $(1 - f_{\mathrm{NDC}}^{\mathrm{sig}})/(1 - f_{\mathrm{NDC}}^{\mathrm{norm}})$ for the NDC background subtraction, and $1 - \sigma_{\mathrm{sig}} \cdot \delta_{\mathrm{sig}}/N_{\mathrm{sig}}$ for the bias correction, where $N_{\mathrm{sig}} \pm \sigma_{\mathrm{sig}} = 360 \pm 22$ and $\delta_{\mathrm{sig}} = 0.09$. The branching-fraction ratio is determined to be

$$\mathcal{R} = 0.525 \pm 0.033, \tag{4}$$

where the uncertainty is due to statistical uncertainties on the efficiency-corrected yields of both the $B^+ \to D_s^+ D_s^- K^+$ and $B^+ \to D^+ D^- K^+$ channels.

VI. SYSTEMATIC UNCERTAINTIES

The sources of the systematic uncertainty on the branching-fraction ratio are summarized in Table I. They can be classified into two categories: the effects on the signal yields and the effects on the efficiencies. The total uncertainty is obtained by adding the contributions in quadrature.

The sources affecting the signal yields include the choice of the signal and background PDFs in the B^+ mass fits,

TABLE I. Sources of systematic uncertainty (syst.) on the branching- fraction ratio. The statistical uncertainty (stat.) is also given.

Systematic source	Relative uncertainty (%)
Signal model	0.3
Background model	0.1
NDC background	2.9
Mass fit bias	0.1
Multiple-candidate removal	0.7
Hardware trigger correction	2.3
PID correction	2.8
Classifier modeling	1.6
Tracking	1.0
Truth matching	0.6
Limited size of simulated samples	0.5
KDE parameters	0.4
Total syst. (stat.)	5.1 (6.3)

the uncertainties on the NDC background fractions in the signal and normalization channels, the uncertainty on the bias of the $B^+ \to D_s^+ D_s^- K^+$ signal yield and the multiple-candidate removal strategy. To evaluate the systematic uncertainty related to the choice of the signal PDF, an alternative model with a Hypatia function [44] is employed in the B^+ mass fits to the signal and normalization channels. The effect due to the choice of the background PDF is evaluated in a similar way, where a second-order polynomial function is used as an alternative. The NDC background fractions in the signal and normalization channels have large uncertainties, which are due to the limited size of the data samples in the $D^{\pm}$ and $D_s^{\pm}$ mass sidebands. These uncertainties are propagated to the branching-fraction ratio. The uncertainty on the bias of the $B^+ \to D_s^+ D_s^- K^+$ signal yield, resulting from the limited number of the pseudoexperiments that are employed to estimate the bias, is propagated in a similar way. Finally, the effect of the multiple-candidate removal strategy is evaluated by retaining an arbitrarily chosen candidate in an event.

The remaining systematic uncertainty sources in Table I influence the efficiencies in the signal and normalization channels. The hardware trigger is generally not well modeled in the LHCb simulation, but the effect is expected to largely cancel in the branching-fraction ratio thanks to the similarity in the topology between the signal and normalization channels. The residual effect is evaluated by applying to the simulated events an event-by-event correction that is determined by calibration samples [45].

The PID response is not well described in the simulation either and thus is corrected in the default result, with the correction determined from calibration samples using the PID transformation approach [34,35]. The performance of the correction is limited by the size of the calibration samples, the choice of the values of hyperparameters in the transformation approach, and the choice of the correction approach itself. The corresponding effects are investigated by extracting the efficiency maps from simulated samples with the correction determined by using alternative calibration samples bootstrapped from the original ones, varying the values of the hyperparameters of the PID transformation approach, and choosing the PID resampling approach [34,35]. The resulting changes on the branching-fraction ratio are taken as the systematic uncertainties and are added in quadrature to obtain the uncertainty due to the imperfect PID correction.

The potentially imperfect descriptions of the discriminating variables in the simulation can cause bias on the efficiencies of the BDTG classifiers. The effect is evaluated by varying the BDTG selection for the two channels and the resulting change of the branching-fraction ratio is taken as the systematic uncertainty.

The uncertainties on the tracking efficiencies for the same species of final-state particles in the signal and

normalization channels are expected to be the same and fully correlated, so their effects on the branching-fraction ratio largely cancel. The residual effect is from different final-state particles in the two channels, i.e. $D_s^+ \to K^- K^+ \pi^+$ and $D^+ \to K^- \pi^+ \pi^+$. The systematic uncertainty on the branching-fraction ratio is evaluated as 1.0% [46,47].

In the simulation, a truth-matching algorithm is used to identify signal decays. The efficiency of this algorithm is not 100%, leading to an underestimation of the efficiencies shown in Fig. 4. However, the truth-matching efficiencies are expected to be very similar between the signal and normalization channels, and thus the associated systematic uncertainties largely cancel. To evaluate the potential residual effect, the truth-matching efficiencies in the two channels are estimated using B^+ mass fits to the simulated samples with and without truth matching. The efficiencies are introduced as correction factors to the branching-fraction ratio, and the resulting variation is taken as the systematic uncertainty.

The kernel width in the KDE method is chosen to be 2 GeV^2 in the default result. To evaluate the systematic effect due to this choice, two alternative values, 1 and 3 GeV^2, are taken in the efficiency parametrizations. The maximum change of the branching-fraction ratio is taken as the systematic uncertainty.

The last systematic uncertainty source affecting the efficiencies is the limited size of simulated samples. The uncertainty is propagated to the branching-fraction ratio using the bootstrap method [48]. Bootstrapped samples are produced by randomly selecting from the simulated candidates with replacements. Each such sample has the same size as the original simulated sample. These samples are employed to determine efficiencies and finally to obtain a set of branching-fraction ratios, whose standard deviation is taken as the systematic uncertainty.

VII. SUMMARY

In conclusion, the $B^+ \to D_s^+ D_s^- K^+$ decay is observed for the first time using the proton-proton collision data collected by the LHCb detector at center-of-mass energies of 7, 8, and 13 TeV, corresponding to an integrated luminosity of 9 fb^{-1}. The significance of the signal observed is larger than 10σ. The branching fraction of this decay is measured relative to that of the $B^+ \to D^+ D^- K^+$ normalization channel as

$$\mathcal{R} = \frac{\mathcal{B}(B^+ \to D_s^+ D_s^- K^+)}{\mathcal{B}(B^+ \to D^+ D^- K^+)}$$
$$= 0.525 \pm 0.033 \pm 0.027 \pm 0.034. \quad (5)$$

With $\mathcal{B}(B^+ \to D^+ D^- K^+) = (2.2 \pm 0.7) \times 10^{-4}$ as the input [11,14], the $B^+ \to D_s^+ D_s^- K^+$ branching fraction is then determined to be

$$\mathcal{B}(B^+ \to D_s^+ D_s^- K^+) = (1.15 \pm 0.07 \pm 0.06 \pm 0.38) \times 10^{-4}. \quad (6)$$

In each of these results, the first and second uncertainties are statistical and systematic, respectively, and the third is from the uncertainties on the known branching fractions of the $D^+ \to K^- \pi^+ \pi^+$ [49], $D_s^+ \to K^- K^+ \pi^+$ [14,50–52], and $B^+ \to D^+ D^- K^+$ decays [11].

The observation of the $B^+ \to D_s^+ D_s^- K^+$ decay fills a major experimental gap in knowledge of the Cabibbo-favored $\bar{b} \to \bar{c}c\bar{s}$ transition with two open-charm hadrons in the final states [14]. The measurement of its branching fraction is of great importance for investigations of the intermediate resonant states. In particular, it is vital input to studies probing the nature of the near-threshold structure in the $D_s^+ D_s^-$ system [16].

[1] B. Aubert *et al.* (*BABAR* Collaboration), Study of resonances in exclusive *B* decays to $\bar{D}^{(*)}D^{(*)}K$, Phys. Rev. D **77,** 011102 (2008).

[2] J. Brodzicka *et al.* (Belle Collaboration), Observation of a New $D_{(sJ)}$ Meson in $B^+ \to \bar{D}^0 D^0 K^+$ Decays, Phys. Rev. Lett. **100,** 092001 (2008).

[3] T. Aushev *et al.* (Belle Collaboration), Study of the decays $B \to D_{s1}(2536)^+ \bar{D}^{(*)}$, Phys. Rev. D **83,** 051102 (2011).

[4] J. P. Lees *et al.* (*BABAR* Collaboration), Dalitz plot analyses of $B^0 \to D^- D^0 K^+$ and $B^+ \to \bar{D}^0 D^0 K^+$ decays, Phys. Rev. D **91,** 052002 (2015).

[5] R. Aaij *et al.* (LHCb Collaboration), Model-Independent Study of Structure in $B^+ \to D^+ D^- K^+$ Decays, Phys. Rev. Lett. **125,** 242001 (2020).

[6] R. Aaij *et al.* (LHCb Collaboration), Amplitude analysis of the $B^+ \to D^+ D^- K^+$ decay, Phys. Rev. D **102,** 112003 (2020).

[7] R. Aaij *et al.* (LHCb Collaboration), Observation of a New Excited D_s^+ State in $B^0 \to D^- D^+ K^+ \pi^-$ Decays, Phys. Rev. Lett. **126,** 122002 (2021).

[8] A. Khodjamirian, T. Mannel, A. A. Pivovarov, and Y.-M. Wang, Charm-loop effect in $B \to K^{(*)} \ell^+ \ell^-$ and $B \to K^* \gamma$, J. High Energy Phys. 09 (2010) 089.

[9] R. Barate *et al.* (ALEPH Collaboration), Observation of doubly charmed *B* decays at LEP, Eur. Phys. J. C **4,** 387 (1998).

[10] B. Aubert *et al.* (*BABAR* Collaboration), Measurement of the branching fractions for the exclusive decays of B^0 and B^+ to $\bar{D}^{(*)} D^{(*)} K$, Phys. Rev. D **68,** 092001 (2003).

[11] P. del Amo Sanchez *et al.* (*BABAR* Collaboration), Measurement of the $B \to \bar{D}^{(*)} D^{(*)} K$ branching fractions, Phys. Rev. D **83,** 032004 (2011).

[12] R. Aaij *et al.* (LHCb Collaboration), First observation of the decay $B^0 \to D^0 \bar{D}^0 K^+ \pi^-$, Phys. Rev. D **102,** 051102 (2020).

[13] R. Aaij *et al.* (LHCb Collaboration), Measurement of branching fraction ratios for $B^+ \to D^{*+} D^- K^+$, $B^+ \to D^{*-} D^+ K^+$, and $B^0 \to D^{*-} D^0 K^+$ decays, J. High Energy Phys. 12 (2020) 139.

[14] P. A. Zyla *et al.* (Particle Data Group), Review of particle physics, Prog. Theor. Exp. Phys. **2020,** 083C01 (2020).

[15] R. Aaij *et al.* (LHCb Collaboration), Observation of New Resonances Decaying to $J/\psi K^+$ and $J/\psi \phi$, Phys. Rev. Lett. **127,** 082001 (2021).

[16] R. Aaij *et al.* (LHCb Collaboration), Companion Letter, Observation of a Resonant Structure Near the $D_s^+ D_s^-$ Threshold in the $B^+ \to D_s^+ D_s^- K^+$ Decay, Phys. Rev. Lett. **131,** 071901 (2023).

[17] A. A. Alves, Jr. *et al.* (LHCb Collaboration), The LHCb detector at the LHC, J. Instrum. **3,** S08005 (2008).

[18] LHCb Collaboration, LHCb detector performance, Int. J. Mod. Phys. A **30,** 1530022 (2015).

[19] R. Aaij *et al.*, Performance of the LHCb vertex locator, J. Instrum. **9,** P09007 (2014).

[20] R. Arink *et al.*, Performance of the LHCb outer tracker, J. Instrum. **9,** P01002 (2014).

[21] P. d'Argent *et al.*, Improved performance of the LHCb outer tracker in LHC Run 2, J. Instrum. **12,** P11016 (2017).

[22] M. Adinolfi *et al.*, Performance of the LHCb RICH detector at the LHC, Eur. Phys. J. C **73,** 2431 (2013).

[23] A. A. Alves, Jr. *et al.*, Performance of the LHCb muon system, J. Instrum. **8,** P02022 (2013).

[24] R. Aaij *et al.*, The LHCb trigger and its performance in 2011, J. Instrum. **8,** P04022 (2013).

[25] V. V. Gligorov and M. Williams, Efficient, reliable and fast high-level triggering using a bonsai boosted decision tree, J. Instrum. **8,** P02013 (2013).

[26] T. Likhomanenko, P. Ilten, E. Khairullin, A. Rogozhnikov, A. Ustyuzhanin, and M. Williams, LHCb topological trigger reoptimization, J. Phys. Conf. Ser. **664,** 082025 (2015).

[27] T. Sjöstrand, S. Mrenna, and P. Skands, A brief introduction to PYTHIA 8.1, Comput. Phys. Commun. **178,** 852 (2008); T. Sjöstrand, S. Mrenna, and P. Skands, PYTHIA 6.4 physics and manual, J. High Energy Phys. 05 (2006) 026.

[28] I. Belyaev *et al.*, Handling of the generation of primary events in Gauss, the LHCb simulation framework, J. Phys. Conf. Ser. **331,** 032047 (2011).

[29] D. J. Lange, The EvtGen particle decay simulation package, Nucl. Instrum. Methods Phys. Res., Sect. A **462,** 152 (2001).

[30] N. Davidson, T. Przedzinski, and Z. Was, PHOTOS interface in C++: Technical and physics documentation, Comput. Phys. Commun. **199,** 86 (2016).

[31] J. Allison *et al.* (Geant4 Collaboration), GEANT4 developments and applications, IEEE Trans. Nucl. Sci. **53,** 270 (2006); S. Agostinelli *et al.* (Geant4 Collaboration), GEANT4: A simulation toolkit, Nucl. Instrum. Methods Phys. Res., Sect. A **506,** 250 (2003).

[32] M. Clemencic, G. Corti, S. Easo, C. R. Jones, S. Miglioranzi, M. Pappagallo, and P Robbe, The LHCb simulation application, Gauss: Design, evolution and experience, J. Phys. Conf. Ser. **331,** 032023 (2011).

[33] D. Müller, M. Clemencic, G. Corti, and M. Gersabeck, ReDecay: A novel approach to speed up the simulation at LHCb, Eur. Phys. J. C **78,** 1009 (2018).

[34] L. Anderlini *et al.*, The PIDCalib package, Report No. LHCb-PUB-2016-021, 2016.

[35] R. Aaij *et al.*, Selection and processing of calibration samples to measure the particle identification performance of the LHCb experiment in Run 2, Eur. Phys. J Tech. Instrum. **6,** 1 (2019).

[36] W. D. Hulsbergen, Decay chain fitting with a Kalman filter, Nucl. Instrum. Methods Phys. Res., Sect. A **552,** 566 (2005).

[37] L. Breiman, J. H. Friedman, R. A. Olshen, and C. J. Stone, *Classification and Regression Trees* (Wadsworth International Group, Belmont, California, USA, 1984).

[38] Y. Freund and R. E. Schapire, A decision-theoretic generalization of on-line learning and an application to boosting, J. Comput. Syst. Sci. **55,** 119 (1997).

[39] H. Voss, A. Hoecker, J. Stelzer, and F. Tegenfeldt, TMVA—Toolkit for multivariate data analysis with ROOT, Proc. Sci. ACAT2007 (**2007**) 040; A. Hoecker *et al.*, TMVA 4—Toolkit for multivariate data analysis with ROOT, users guide, arXiv:physics/0703039.

[40] T. Skwarnicki, A study of the radiative cascade transitions between the upsilon-prime and upsilon resonances, Ph.D. thesis, Institute of Nuclear Physics, Krakow, 1986.

[41] S. S. Wilks, The large-sample distribution of the likelihood ratio for testing composite hypotheses, Ann. Math. Stat. **9**, 60 (1938).

[42] M. Pivk and F. R. Le Diberder, *sPlot*: A statistical tool to unfold data distributions, Nucl. Instrum. Methods Phys. Res., Sect. A **555**, 356 (2005).

[43] A. Poluektov, Kernel density estimation of a multidimensional efficiency profile, J. Instrum. **10**, P02011 (2015).

[44] D. Martínez Santos and F. Dupertuis, Mass distributions marginalized over per-event errors, Nucl. Instrum. Methods Phys. Res., Sect. A **764**, 150 (2014).

[45] A. Martin Sanchez, P. Robbe, and M.-H. Schune, Performances of the LHCb L0 calorimeter trigger, Report No. LHCb-PUB-2011-026, No. CERN-LHCb-PUB-2011-026, 2012.

[46] R. Aaij *et al.* (LHCb Collaboration), Measurement of the branching fraction and *CP* asymmetry in $B^+ \to J/\psi\rho^+$ decays, Eur. Phys. J. C **79**, 537 (2019).

[47] R. Aaij *et al.* (LHCb Collaboration), Measurement of the branching fraction of the $B^0 \to D_s^+ \pi^-$ decay, Eur. Phys. J. C **81**, 314 (2021).

[48] B. Efron, Bootstrap methods: Another look at the jackknife, Ann. Stat. **7**, 1 (1979).

[49] G. Bonvicini *et al.* (CLEO Collaboration), Updated measurements of absolute D^+ and D^0 hadronic branching fractions and $\sigma(e^+e^- \to D\bar{D})$ at $E_{cm} = 3774$ MeV, Phys. Rev. D **89**, 072002 (2014); G. Bonvicini *et al.* (CLEO Collaboration), Phys. Rev. D**91**, 019903(E) (2015).

[50] P. del Amo Sanchez *et al.* (*BABAR* Collaboration), Measurement of the absolute branching fractions for $D_s^- \to \ell^- \bar{\nu}_\ell$ and extraction of the decay constant f_{D_s}, Phys. Rev. D **82**, 091103 (2010); **91**, 019901(E) (2015).

[51] P. U. E. Onyisi *et al.* (CLEO Collaboration), Improved measurement of absolute hadronic branching fractions of the D_s^+ meson, Phys. Rev. D **88**, 032009 (2013).

[52] A. Zupanc *et al.* (Belle Collaboration), Measurements of branching fractions of leptonic and hadronic D_s^+ meson decays and extraction of the D_s^+ meson decay constant, J. High Energy Phys. 09 (2013) 139.

R. Aaij[32] A. S. W. Abdelmotteleb[50] C. Abellan Beteta,[44] F. Abudinén[50] T. Ackernley[54] B. Adeva[40] M. Adinolfi[48] H. Afsharnia,[9] C. Agapopoulou[13] C. A. Aidala[77] S. Aiola[25] Z. Ajaltouni[9] S. Akar[59] K. Akiba[32] J. Albrecht[15] F. Alessio[42] M. Alexander[53] A. Alfonso Albero[39] Z. Aliouche[56] P. Alvarez Cartelle[49] R. Amalric[13] S. Amato[2] J. L. Amey[48] Y. Amhis[11,42] L. An[42] L. Anderlini[22] M. Andersson[44] A. Andreianov[38] M. Andreotti[21] D. Andreou[62] D. Ao[6] F. Archilli[17] A. Artamonov[38] M. Artuso[62] E. Aslanides[10] M. Atzeni[44] B. Audurier[12] S. Bachmann[17] M. Bachmayer[43] J. J. Back[50] A. Bailly-reyre,[13] P. Baladron Rodriguez[40] V. Balagura[12] W. Baldini[21] J. Baptista de Souza Leite[1] M. Barbetti[22,j] R. J. Barlow[56] S. Barsuk[11] W. Barter[55] M. Bartolini[49] F. Baryshnikov[38] J. M. Basels[14] G. Bassi[29,p] B. Batsukh[4] A. Battig[15] A. Bay[43] A. Beck[50] M. Becker[15] F. Bedeschi[29] I. B. Bediaga[1] A. Beiter[62] V. Belavin,[38] S. Belin[40] V. Bellee[44] K. Belous[38] I. Belov[38] I. Belyaev[38] G. Benane[10] G. Bencivenni[23] E. Ben-Haim[13] A. Berezhnoy[38] R. Bernet[44] S. Bernet Andres[75] D. Berninghoff,[17] H. C. Bernstein[62] C. Bertella[56] A. Bertolin[28] C. Betancourt[44] F. Betti[42] Ia. Bezshyiko[44] S. Bhasin[48] J. Bhom[35] L. Bian[68] M. S. Bieker[15] N. V. Biesuz[21] S. Bifani[47] P. Billoir[13] A. Biolchini[32] M. Birch[55] F. C. R. Bishop[49] A. Bitadze[56] A. Bizzeti[] M. P. Blago[49] T. Blake[50] F. Blanc[43] S. Blusk[62] D. Bobulska[53] J. A. Boelhauve[15] O. Boente Garcia[12] T. Boettcher[59] A. Boldyrev[38] C. S. Bolognani[74] R. Bolzonella[21,i] N. Bondar[38,42] F. Borgato[28] S. Borghi[56] M. Borsato[17] J. T. Borsuk[35] S. A. Bouchiba[43] T. J. V. Bowcock[54] A. Boyer[42] C. Bozzi[21] M. J. Bradley[55] S. Braun[60] A. Brea Rodriguez[40] J. Brodzicka[35] A. Brossa Gonzalo[40] J. Brown[54] D. Brundu[27] A. Buonaura[44] L. Buonincontri[28] A. T. Burke[56] C. Burr[42] A. Bursche[66] A. Butkevich[38] J. S. Butter[32] J. Buytaert[42] W. Byczynski[42] S. Cadeddu[27] H. Cai[68] R. Calabrese[21,i] L. Calefice[15] S. Cali[23] R. Calladine[47] M. Calvi[26,m] M. Calvo Gomez[75] P. Campana[23] D. H. Campora Perez[74] A. F. Campoverde Quezada[6] S. Capelli[26,m] L. Capriotti[20,g] A. Carbone[20,g] G. Carboni[31] R. Cardinale[24,k] A. Cardini[27] I. Carli[4] P. Carniti[26,m] L. Carus,[14] A. Casais Vidal[40] R. Caspary[17] G. Casse[54] M. Cattaneo[42] G. Cavallero[42] V. Cavallini[21,i] S. Celani[43] J. Cerasoli[10] D. Cervenkov[57] A. J. Chadwick[54] M. G. Chapman,[48] M. Charles[13] Ph. Charpentier[42] C. A. Chavez Barajas[54] M. Chefdeville[8] C. Chen[3] S. Chen[4] A. Chernov[35] S. Chernyshenko[46] V. Chobanova[40] S. Cholak[43] M. Chrzaszcz[35] A. Chubykin[38] V. Chulikov[38] P. Ciambrone[23] M. F. Cicala[50] X. Cid Vidal[40] G. Ciezarek[42] G. Ciullo[21,i] P. E. L. Clarke[52] M. Clemencic[42] H. V. Cliff[49] J. Closier[42] J. L. Cobbledick[56] V. Coco[42] J. A. B. Coelho[11] J. Cogan[10] E. Cogneras[9] L. Cojocariu[37] P. Collins[42] T. Colombo[42] L. Congedo[19] A. Contu[27] N. Cooke[47] I. Corredoira[40] G. Corti[42] B. Couturier[42] D. C. Craik[58] J. Crkovská[61] M. Cruz Torres[1,e] R. Currie[52] C. L. Da Silva[61] S. Dadabaev[38] L. Dai[65]

X. Dai[5], E. Dall'Occo[15], J. Dalseno[40], C. D'Ambrosio[42], J. Daniel[9], A. Danilina[38], P. d'Argent[15], J. E. Davies[56], A. Davis[56], O. De Aguiar Francisco[56], J. de Boer[42], K. De Bruyn[73], S. De Capua[56], M. De Cian[43], U. De Freitas Carneiro Da Graca[1], E. De Lucia[23], J. M. De Miranda[1], L. De Paula[2], M. De Serio[19,f], D. De Simone[44], P. De Simone[23], F. De Vellis[15], J. A. de Vries[74], C. T. Dean[61], F. Debernardis[19,f], D. Decamp[8], V. Dedu[10], L. Del Buono[13], B. Delaney[58], H.-P. Dembinski[15], V. Denysenko[44], O. Deschamps[9], F. Dettori[27,h], B. Dey[71], A. Di Cicco[23], P. Di Nezza[23], I. Diachkov[38], S. Didenko[38], L. Dieste Maronas[40], S. Ding[62], V. Dobishuk[46], A. Dolmatov[38], C. Dong[3], A. M. Donohoe[18], F. Dordei[27], A. C. dos Reis[1], L. Douglas[53], A. G. Downes[8], M. W. Dudek[35], L. Dufour[42], V. Duk[72], P. Durante[42], J. M. Durham[61], D. Dutta[56], A. Dziurda[35], A. Dzyuba[38], S. Easo[51], U. Egede[63], V. Egorychev[38], S. Eidelman,[38,†] C. Eirea Orro[40], S. Eisenhardt[52], E. Ejopu[56], S. Ek-In[43], L. Eklund[76], S. Ely[62], A. Ene[37], E. Epple[61], S. Escher[14], J. Eschle[44], S. Esen[44], T. Evans[56], F. Fabiano[27,h], L. N. Falcao[1], Y. Fan[6], B. Fang[68], S. Farry[54], D. Fazzini[26,m], M. Feo[42], M. Fernandez Gomez[40], A. D. Fernez[60], F. Ferrari[20], L. Ferreira Lopes[43], F. Ferreira Rodrigues[2], S. Ferreres Sole[32], M. Ferrillo[44], M. Ferro-Luzzi[42], S. Filippov[38], R. A. Fini[19], M. Fiorini[21,i], M. Firlej[34], K. M. Fischer[57], D. S. Fitzgerald[77], C. Fitzpatrick[56], T. Fiutowski[34], F. Fleuret[12], M. Fontana[13], F. Fontanelli[24,k], R. Forty[42], D. Foulds-Holt[49], V. Franco Lima[54], M. Franco Sevilla[60], M. Frank[42], E. Franzoso[21,i], G. Frau[17], C. Frei[42], D. A. Friday[53], J. Fu[6], Q. Fuehring[15], T. Fulghesu[13], E. Gabriel[32], G. Galati[19,f], M. D. Galati[73], A. Gallas Torreira[40], D. Galli[20,g], S. Gambetta[52,42], Y. Gan[3], M. Gandelman[2], P. Gandini[25], Y. Gao[5], M. Garau[27,h], L. M. Garcia Martin[50], P. Garcia Moreno[39], J. García Pardiñas[26,m], B. Garcia Plana,[40] F. A. Garcia Rosales[12], L. Garrido[39], C. Gaspar[42], R. E. Geertsema[32], D. Gerick,[17] L. L. Gerken[15], E. Gersabeck[56], M. Gersabeck[56], T. Gershon[50], L. Giambastiani[28], V. Gibson[49], H. K. Giemza[36], A. L. Gilman[57], M. Giovannetti[23,s], A. Gioventù[40], P. Gironella Gironell[39], C. Giugliano[21,i], M. A. Giza[35], K. Gizdov[52], E. L. Gkougkousis[42], V. V. Gligorov[13,42], C. Göbel[64], E. Golobardes[75], D. Golubkov[38], A. Golutvin[55,38], A. Gomes[1,a], S. Gomez Fernandez[39], F. Goncalves Abrantes[57], M. Goncerz[35], G. Gong[3], I. V. Gorelov[38], C. Gotti[26], J. P. Grabowski[17], T. Grammatico[13], L. A. Granado Cardoso[42], E. Graugés[39], E. Graverini[43], G. Graziani,[ ] A. T. Grecu[37], L. M. Greeven[32], N. A. Grieser[4], L. Grillo[53], S. Gromov[38], B. R. Gruberg Cazon[57], C. Gu[3], M. Guarise[21,i], M. Guittiere[11], P. A. Günther[17], E. Gushchin[38], A. Guth,[14] Y. Guz[38], T. Gys[42], T. Hadavizadeh[63], G. Haefeli[43], C. Haen[42], J. Haimberger[42], S. C. Haines[49], T. Halewood-leagas[54], M. M. Halvorsen[42], P. M. Hamilton[60], J. Hammerich[54], Q. Han[7], X. Han[17], E. B. Hansen[56], S. Hansmann-Menzemer[17,42], L. Hao[6], N. Harnew[57], T. Harrison[54], C. Hasse[42], M. Hatch[42], J. He[6,c], K. Heijhoff[32], K. Heinicke[15], C. Henderson[59], R. D. L. Henderson[63,50], A. M. Hennequin[58], K. Hennessy[54], L. Henry[42], J. H Herd[55], J. Heuel[14], A. Hicheur[2], D. Hill[43], M. Hilton[56], S. E. Hollitt[15], J. Horswill[56], R. Hou[7], Y. Hou[8], J. Hu[17], J. Hu[66], W. Hu[5], X. Hu[3], W. Huang[6], X. Huang,[68] W. Hulsbergen[32], R. J. Hunter[50], M. Hushchyn[38], D. Hutchcroft[54], P. Ibis[15], M. Idzik[34], D. Ilin[38], P. Ilten[59], A. Inglessi[38], A. Iniukhin[38], A. Ishteev[38], K. Ivshin[38], R. Jacobsson[42], H. Jage[14], S. J. Jaimes Elles[41], S. Jakobsen[42], E. Jans[32], B. K. Jashal[41], A. Jawahery[60], V. Jevtic[15], E. Jiang[60], X. Jiang[4,6], Y. Jiang[6], M. John[57], D. Johnson[58], C. R. Jones[49], T. P. Jones[50], B. Jost[42], N. Jurik[42], I. Juszczak[35], S. Kandybei[45], Y. Kang[3], M. Karacson[42], D. Karpenkov[38], M. Karpov[38], J. W. Kautz[59], F. Keizer[42], D. M. Keller[62], M. Kenzie[50], T. Ketel[32], B. Khanji[15], A. Kharisova[38], S. Kholodenko[38], G. Khreich[11], T. Kirn[14], V. S. Kirsebom[43], O. Kitouni[58], S. Klaver[33], N. Kleijne[29,p], K. Klimaszewski[36], M. R. Kmiec[36], S. Koliiev[46], A. Kondybayeva[38], A. Konoplyannikov[38], P. Kopciewicz[34], R. Kopecna,[17] P. Koppenburg[32], M. Korolev[38], I. Kostiuk[32,46], O. Kot,[46] S. Kotriakhova,[ ] A. Kozachuk[38], P. Kravchenko[38], L. Kravchuk[38], R. D. Krawczyk[42], M. Kreps[50], S. Kretzschmar[14], P. Krokovny[38], W. Krupa[34], W. Krzemien[36], J. Kubat,[17] W. Kucewicz[35,34], M. Kucharczyk[35], V. Kudryavtsev[38], G. J. Kunde[61], A. Kupsc[76], D. Lacarrere[42], G. Lafferty[56], A. Lai[27], A. Lampis[27,h], D. Lancierini[44], C. Landesa Gomez[40], J. J. Lane[56], R. Lane[48], G. Lanfranchi[23], C. Langenbruch[14], J. Langer[15], O. Lantwin[38], T. Latham[50], F. Lazzari[29,t], M. Lazzaroni[25], R. Le Gac[10], S. H. Lee[77], R. Lefèvre[9], A. Leflat[38], S. Legotin[38], P. Lenisa[21,i], O. Leroy[10], T. Lesiak[35], B. Leverington[17], A. Li[3], H. Li[66], K. Li[7], P. Li[17], P.-R. Li[67], S. Li[7], T. Li[66], Y. Li[4], Z. Li[62], X. Liang[62], C. Lin[6], T. Lin[51], R. Lindner[42], V. Lisovskyi[15], R. Litvinov[27,h], G. Liu[66], H. Liu[6], Q. Liu[6], S. Liu[4,6], A. Lobo Salvia[39], A. Loi[27], R. Lollini[72], J. Lomba Castro[40], I. Longstaff,[53] J. H. Lopes[2], A. Lopez Huertas[39], S. López Soliño[40], G. H. Lovell[49], Y. Lu[4,b]

C. Lucarelli[22,j] D. Lucchesi[28,n] S. Luchuk[38] M. Lucio Martinez[74] V. Lukashenko[32,46] Y. Luo[3] A. Lupato[56] E. Luppi[21,i] A. Lusiani[29,p] K. Lynch[18] X.-R. Lyu[6] L. Ma[4] R. Ma[6] S. Maccolini[20] F. Machefert[11] F. Maciuc[37] I. Mackay[57] V. Macko[43] P. Mackowiak[15] L. R. Madhan Mohan[48] A. Maevskiy[38] D. Maisuzenko[38] M. W. Majewski[34] J. J. Malczewski[35] S. Malde[57] B. Malecki[35,42] A. Malinin[38] T. Maltsev[38] G. Manca[27,h] G. Mancinelli[10] C. Mancuso[11,25,l] D. Manuzzi[20] C. A. Manzari[44] D. Marangotto[25,l] J. M. Maratas[9,v] J. F. Marchand[8] U. Marconi[20] S. Mariani[22,j] C. Marin Benito[39] J. Marks[17] A. M. Marshall[48] P. J. Marshall[54] G. Martelli[72,o] G. Martellotti[30] L. Martinazzoli[42,m] M. Martinelli[26,m] D. Martinez Santos[40] F. Martinez Vidal[41] A. Massafferri[1] M. Materok[14] R. Matev[42] A. Mathad[44] V. Matiunin[38] C. Matteuzzi[26] K. R. Mattioli[77] A. Mauri[32] E. Maurice[12] J. Mauricio[39] M. Mazurek[42] M. McCann[55] L. Mcconnell[18] T. H. McGrath[56] N. T. McHugh[53] A. McNab[56] R. McNulty[18] J. V. Mead[54] B. Meadows[59] G. Meier[15] D. Melnychuk[36] S. Meloni[26,m] M. Merk[32,74] A. Merli[25,l] L. Meyer Garcia[2] D. Miao[4,6] M. Mikhasenko[70,d] D. A. Milanes[69] E. Millard[50] M. Milovanovic[42] M.-N. Minard[8,†] A. Minotti[26,m] T. Miralles[9] S. E. Mitchell[52] B. Mitreska[56] D. S. Mitzel[15] A. Mödden[15] R. A. Mohammed[57] R. D. Moise[14] S. Mokhnenko[38] T. Mombächer[40] M. Monk[50,63] I. A. Monroy[69] S. Monteil[9] M. Morandin[28] G. Morello[23] M. J. Morello[29,p] J. Moron[34] A. B. Morris[70] A. G. Morris[50] R. Mountain[62] H. Mu[3] E. Muhammad[50] F. Muheim[52] M. Mulder[73] K. Müller[44] C. H. Murphy[57] D. Murray[56] R. Murta[55] P. Muzzetto[27,h] P. Naik[48] T. Nakada[43] R. Nandakumar[51] T. Nanut[42] I. Nasteva[2] M. Needham[52] N. Neri[25,l] S. Neubert[70] N. Neufeld[42] P. Neustroev[38] R. Newcombe[55] J. Nicolini[15,11] E. M. Niel[43] S. Nieswand[14] N. Nikitin[38] N. S. Nolte[58] C. Normand[8,27,h] J. Novoa Fernandez[40] C. Nunez[77] A. Oblakowska-Mucha[34] V. Obraztsov[38] T. Oeser[14] D. P. O'Hanlon[48] S. Okamura[21,i] R. Oldeman[27,h] F. Oliva[52] M. E. Olivares[62] C. J. G. Onderwater[73] R. H. O'Neil[52] J. M. Otalora Goicochea[2] T. Ovsiannikova[38] P. Owen[44] A. Oyanguren[41] O. Ozcelik[52] K. O. Padeken[70] B. Pagare[50] P. R. Pais[42] T. Pajero[57] A. Palano[19] M. Palutan[23] Y. Pan[56] G. Panshin[38] L. Paolucci[50] A. Papanestis[51] M. Pappagallo[19,f] L. L. Pappalardo[21,i] C. Pappenheimer[59] W. Parker[60] C. Parkes[56] B. Passalacqua[21,i] G. Passaleva[22] A. Pastore[19] M. Patel[55] C. Patrignani[20,g] C. J. Pawley[74] A. Pearce[42] A. Pellegrino[32] M. Pepe Altarelli[42] S. Perazzini[20] D. Pereima[38] A. Pereiro Castro[40] P. Perret[9] M. Petric[53] K. Petridis[48] A. Petrolini[24,k] A. Petrov[38] S. Petrucci[52] M. Petruzzo[25] H. Pham[62] A. Philippov[38] R. Piandani[6] L. Pica[29,p] M. Piccini[72] B. Pietrzyk[8] G. Pietrzyk[11] M. Pili[57] D. Pinci[30] F. Pisani[42] M. Pizzichemi[26,42,m] V. Placinta[37] J. Plews[47] M. Plo Casasus[40] F. Polci[13,42] M. Poli Lener[23] M. Poliakova[62] A. Poluektov[10] N. Polukhina[38] I. Polyakov[42] E. Polycarpo[2] S. Ponce[42] D. Popov[6,42] S. Popov[38] S. Poslavskii[38] K. Prasanth[35] L. Promberger[42] C. Prouve[40] V. Pugatch[46] V. Puill[11] G. Punzi[29,q] H. R. Qi[3] W. Qian[6] N. Qin[3] S. Qu[3] R. Quagliani[43] N. V. Raab[18] R. I. Rabadan Trejo[6] B. Rachwal[34] J. H. Rademacker[48] R. Rajagopalan[62] M. Rama[29] M. Ramos Pernas[50] M. S. Rangel[2] F. Ratnikov[38] G. Raven[33,42] M. Rebollo De Miguel[41] F. Redi[42] J. Reich[48] F. Reiss[56] C. Remon Alepuz[41] Z. Ren[3] V. Renaudin[57] P. K. Resmi[10] R. Ribatti[29,p] A. M. Ricci[27] S. Ricciardi[51] K. Richardson[58] M. Richardson-Slipper[52] K. Rinnert[54] P. Robbe[11] G. Robertson[52] A. B. Rodrigues[43] E. Rodrigues[54] E. Rodriguez Fernandez[40] J. A. Rodriguez Lopez[69] E. Rodriguez Rodriguez[40] A. Rollings[57] P. Roloff[42] V. Romanovskiy[38] M. Romero Lamas[40] A. Romero Vidal[40] J. D. Roth[77,†] M. Rotondo[23] M. S. Rudolph[62] T. Ruf[42] R. A. Ruiz Fernandez[40] J. Ruiz Vidal[41] A. Ryzhikov[38] J. Ryzka[34] J. J. Saborido Silva[40] N. Sagidova[38] N. Sahoo[47] B. Saitta[27,h] M. Salomoni[42] C. Sanchez Gras[32] I. Sanderswood[41] R. Santacesaria[30] C. Santamarina Rios[40] M. Santimaria[23] E. Santovetti[31,s] D. Saranin[38] G. Sarpis[14] M. Sarpis[70] A. Sarti[30] C. Satriano[30,r] A. Satta[31] M. Saur[15] D. Savrina[38] H. Sazak[9] L. G. Scantlebury Smead[57] A. Scarabotto[13] S. Schael[14] S. Scherl[54] M. Schiller[53] H. Schindler[42] M. Schmelling[16] B. Schmidt[42] S. Schmitt[14] O. Schneider[43] A. Schopper[42] M. Schubiger[32] S. Schulte[43] M. H. Schune[11] R. Schwemmer[42] B. Sciascia[23,42] A. Sciuccati[42] S. Sellam[40] A. Semennikov[38] M. Senghi Soares[33] A. Sergi[24,k] N. Serra[44] L. Sestini[28] A. Seuthe[15] Y. Shang[5] D. M. Shangase[77] M. Shapkin[38] I. Shchemerov[38] L. Shchutska[43] T. Shears[54] L. Shekhtman[38] Z. Shen[5] S. Sheng[4,6] V. Shevchenko[38] B. Shi[6] E. B. Shields[26,m] Y. Shimizu[11] E. Shmanin[38] J. D. Shupperd[62] B. G. Siddi[21,i] R. Silva Coutinho[44] G. Simi[28] S. Simone[19,f] M. Singla[63] N. Skidmore[56] R. Skuza[17] T. Skwarnicki[62] M. W. Slater[47] J. C. Smallwood[57] J. G. Smeaton[49] E. Smith[44] K. Smith[61] M. Smith[55] A. Snoch[32]

L. Soares Lavra[9], M. D. Sokoloff[59], F. J. P. Soler[53], A. Solomin[38,48], A. Solovev[38], I. Solovyev[38], R. Song[63], F. L. Souza De Almeida[2], B. Souza De Paula[2], B. Spaan[15,†], E. Spadaro Norella[25,l], E. Spiridenkov[38], P. Spradlin[53], V. Sriskaran[42], F. Stagni[42], M. Stahl[59], S. Stahl[42], S. Stanislaus[57], E. N. Stein[42], O. Steinkamp[44], O. Stenyakin[38], H. Stevens[15], S. Stone[62,†], D. Strekalina[38], F. Suljik[57], J. Sun[27], L. Sun[68], Y. Sun[60], P. Svihra[56], P. N. Swallow[47], K. Swientek[34], A. Szabelski[36], T. Szumlak[34], M. Szymanski[42], Y. Tan[3], S. Taneja[56], A. R. Tanner[48], M. D. Tat[57], A. Terentev[38], F. Teubert[42], E. Thomas[42], D. J. D. Thompson[47], K. A. Thomson[54], H. Tilquin[55], V. Tisserand[9], S. T'Jampens[8], M. Tobin[4], L. Tomassetti[21,i], G. Tonani[25,l], X. Tong[5], D. Torres Machado[1], D. Y. Tou[3], E. Trifonova[38], S. M. Trilov[48], C. Trippl[43], G. Tuci[6], A. Tully[43], N. Tuning[32], A. Ukleja[36], D. J. Unverzagt[17], E. Ursov[38], A. Usachov[32], A. Ustyuzhanin[38], U. Uwer[17], A. Vagner[38], V. Vagnoni[20], A. Valassi[42], G. Valenti[20], N. Valls Canudas[75], M. van Beuzekom[32], M. Van Dijk[43], H. Van Hecke[61], E. van Herwijnen[38], C. B. Van Hulse[40,w], M. van Veghel[73], R. Vazquez Gomez[39], P. Vazquez Regueiro[40], C. Vázquez Sierra[42], S. Vecchi[21], J. J. Velthuis[48], M. Veltri[22,u], A. Venkateswaran[43], M. Veronesi[32], M. Vesterinen[50], D. Vieira[59], M. Vieites Diaz[43], X. Vilasis-Cardona[75], E. Vilella Figueras[54], A. Villa[20], P. Vincent[13], F. C. Volle[11], D. vom Bruch[10], A. Vorobyev[38], V. Vorobyev[38], N. Voropaev[38], K. Vos[74], C. Vrahas[52], R. Waldi[17], J. Walsh[29], G. Wan[5], C. Wang[17], J. Wang[5], J. Wang[4], J. Wang[3], J. Wang[68], M. Wang[5], R. Wang[48], X. Wang[66], Y. Wang[7], Z. Wang[44], Z. Wang[3], Z. Wang[6], J. A. Ward[50,63], N. K. Watson[47], D. Websdale[55], Y. Wei[5], C. Weisser[58], B. D. C. Westhenry[48], D. J. White[56], M. Whitehead[53], A. R. Wiederhold[50], D. Wiedner[15], G. Wilkinson[57], M. K. Wilkinson[59], I. Williams[49], M. Williams[58], M. R. J. Williams[52], R. Williams[49], F. F. Wilson[51], W. Wislicki[36], M. Witek[35], L. Witola[17], C. P. Wong[61], G. Wormser[11], S. A. Wotton[49], H. Wu[62], K. Wyllie[42], Z. Xiang[6], D. Xiao[7], Y. Xie[7], A. Xu[5], J. Xu[6], L. Xu[3], L. Xu[3], M. Xu[50], Q. Xu[6], Z. Xu[9], Z. Xu[6], D. Yang[3], S. Yang[6], Y. Yang[6], Z. Yang[5], Z. Yang[60], L. E. Yeomans[54], V. Yeroshenko[11], H. Yeung[56], H. Yin[7], J. Yu[65], X. Yuan[62], E. Zaffaroni[43], M. Zavertyaev[16], M. Zdybal[35], O. Zenaiev[42], M. Zeng[3], C. Zhang[5], D. Zhang[7], L. Zhang[3], S. Zhang[65], S. Zhang[5], Y. Zhang[5], Y. Zhang[57], A. Zharkova[38], A. Zhelezov[17], Y. Zheng[6], T. Zhou[5], X. Zhou[6], Y. Zhou[6], V. Zhovkovska[11], X. Zhu[3], X. Zhu[7], Z. Zhu[6], V. Zhukov[14,38], Q. Zou[4,6], S. Zucchelli[20,g], D. Zuliani[28], and G. Zunica[56]

(LHCb Collaboration)

[1]*Centro Brasileiro de Pesquisas Físicas (CBPF), Rio de Janeiro, Brazil*
[2]*Universidade Federal do Rio de Janeiro (UFRJ), Rio de Janeiro, Brazil*
[3]*Center for High Energy Physics, Tsinghua University, Beijing, China*
[4]*Institute Of High Energy Physics (IHEP), Beijing, China*
[5]*School of Physics State Key Laboratory of Nuclear Physics and Technology,*
Peking University, Beijing, China
[6]*University of Chinese Academy of Sciences, Beijing, China*
[7]*Institute of Particle Physics, Central China Normal University, Wuhan, Hubei, China*
[8]*Université Savoie Mont Blanc, CNRS, IN2P3-LAPP, Annecy, France*
[9]*Université Clermont Auvergne, CNRS/IN2P3, LPC, Clermont-Ferrand, France*
[10]*Aix Marseille Univ, CNRS/IN2P3, CPPM, Marseille, France*
[11]*Université Paris-Saclay, CNRS/IN2P3, IJCLab, Orsay, France*
[12]*Laboratoire Leprince-Ringuet, CNRS/IN2P3, Ecole Polytechnique,*
Institut Polytechnique de Paris, Palaiseau, France
[13]*LPNHE, Sorbonne Université, Paris Diderot Sorbonne Paris Cité, CNRS/IN2P3, Paris, France*
[14]*I. Physikalisches Institut, RWTH Aachen University, Aachen, Germany*
[15]*Fakultät Physik, Technische Universität Dortmund, Dortmund, Germany*
[16]*Max-Planck-Institut für Kernphysik (MPIK), Heidelberg, Germany*
[17]*Physikalisches Institut, Ruprecht-Karls-Universität Heidelberg, Heidelberg, Germany*
[18]*School of Physics, University College Dublin, Dublin, Ireland*
[19]*INFN Sezione di Bari, Bari, Italy*
[20]*INFN Sezione di Bologna, Bologna, Italy*
[21]*INFN Sezione di Ferrara, Ferrara, Italy*
[22]*INFN Sezione di Firenze, Firenze, Italy*
[23]*INFN Laboratori Nazionali di Frascati, Frascati, Italy*
[24]*INFN Sezione di Genova, Genova, Italy*

[25]*INFN Sezione di Milano, Milano, Italy*
[26]*INFN Sezione di Milano-Bicocca, Milano, Italy*
[27]*INFN Sezione di Cagliari, Monserrato, Italy*
[28]*Università degli Studi di Padova, Università e INFN, Padova, Padova, Italy*
[29]*INFN Sezione di Pisa, Pisa, Italy*
[30]*INFN Sezione di Roma La Sapienza, Roma, Italy*
[31]*INFN Sezione di Roma Tor Vergata, Roma, Italy*
[32]*Nikhef National Institute for Subatomic Physics, Amsterdam, Netherlands*
[33]*Nikhef National Institute for Subatomic Physics and VU University Amsterdam, Amsterdam, Netherlands*
[34]*AGH - University of Science and Technology, Faculty of Physics and Applied Computer Science, Kraków, Poland*
[35]*Henryk Niewodniczanski Institute of Nuclear Physics Polish Academy of Sciences, Kraków, Poland*
[36]*National Center for Nuclear Research (NCBJ), Warsaw, Poland*
[37]*Horia Hulubei National Institute of Physics and Nuclear Engineering, Bucharest-Magurele, Romania*
[38]*Affiliated with an institute covered by a cooperation agreement with CERN*
[39]*ICCUB, Universitat de Barcelona, Barcelona, Spain*
[40]*Instituto Galego de Física de Altas Enerxías (IGFAE), Universidade de Santiago de Compostela, Santiago de Compostela, Spain*
[41]*Instituto de Fisica Corpuscular, Centro Mixto Universidad de Valencia - CSIC, Valencia, Spain*
[42]*European Organization for Nuclear Research (CERN), Geneva, Switzerland*
[43]*Institute of Physics, Ecole Polytechnique Fédérale de Lausanne (EPFL), Lausanne, Switzerland*
[44]*Physik-Institut, Universität Zürich, Zürich, Switzerland*
[45]*NSC Kharkiv Institute of Physics and Technology (NSC KIPT), Kharkiv, Ukraine*
[46]*Institute for Nuclear Research of the National Academy of Sciences (KINR), Kyiv, Ukraine*
[47]*University of Birmingham, Birmingham, United Kingdom*
[48]*H.H. Wills Physics Laboratory, University of Bristol, Bristol, United Kingdom*
[49]*Cavendish Laboratory, University of Cambridge, Cambridge, United Kingdom*
[50]*Department of Physics, University of Warwick, Coventry, United Kingdom*
[51]*STFC Rutherford Appleton Laboratory, Didcot, United Kingdom*
[52]*School of Physics and Astronomy, University of Edinburgh, Edinburgh, United Kingdom*
[53]*School of Physics and Astronomy, University of Glasgow, Glasgow, United Kingdom*
[54]*Oliver Lodge Laboratory, University of Liverpool, Liverpool, United Kingdom*
[55]*Imperial College London, London, United Kingdom*
[56]*Department of Physics and Astronomy, University of Manchester, Manchester, United Kingdom*
[57]*Department of Physics, University of Oxford, Oxford, United Kingdom*
[58]*Massachusetts Institute of Technology, Cambridge, Massachusetts, USA*
[59]*University of Cincinnati, Cincinnati, Ohio, USA*
[60]*University of Maryland, College Park, Maryland, USA*
[61]*Los Alamos National Laboratory (LANL), Los Alamos, New Mexico, USA*
[62]*Syracuse University, Syracuse, New York, USA*
[63]*School of Physics and Astronomy, Monash University, Melbourne, Australia (associated with Department of Physics, University of Warwick, Coventry, United Kingdom)*
[64]*Pontifícia Universidade Católica do Rio de Janeiro (PUC-Rio), Rio de Janeiro, Brazil (associated with Universidade Federal do Rio de Janeiro (UFRJ), Rio de Janeiro, Brazil)*
[65]*Physics and Micro Electronic College, Hunan University, Changsha City, China (associated with Institute of Particle Physics, Central China Normal University, Wuhan, Hubei, China)*
[66]*Guangdong Provincial Key Laboratory of Nuclear Science, Guangdong-Hong Kong Joint Laboratory of Quantum Matter, Institute of Quantum Matter, South China Normal University, Guangzhou, China (associated with Center for High Energy Physics, Tsinghua University, Beijing, China)*
[67]*Lanzhou University, Lanzhou, China (associated with Institute of High Energy Physics (IHEP), Beijing, China)*
[68]*School of Physics and Technology, Wuhan University, Wuhan, China (associated with Center for High Energy Physics, Tsinghua University, Beijing, China)*
[69]*Departamento de Fisica, Universidad Nacional de Colombia, Bogota, Colombia (associated with LPNHE, Sorbonne Université, Paris Diderot Sorbonne Paris Cité, CNRS/IN2P3, Paris, France)*
[70]*Universität Bonn - Helmholtz-Institut für Strahlen und Kernphysik, Bonn, Germany (associated with Physikalisches Institut, Ruprecht-Karls-Universität Heidelberg, Heidelberg, Germany)*
[71]*Eotvos Lorand University, Budapest, Hungary (associated with European Organization for Nuclear Research (CERN), Geneva, Switzerland)*
[72]*INFN Sezione di Perugia, Perugia, Italy (associated with INFN Sezione di Ferrara, Ferrara, Italy)*

[73]*Van Swinderen Institute, University of Groningen, Groningen, Netherlands (associated with Nikhef National Institute for Subatomic Physics, Amsterdam, Netherlands)*

[74]*Universiteit Maastricht, Maastricht, Netherlands (associated with Nikhef National Institute for Subatomic Physics, Amsterdam, Netherlands)*

[75]*DS4DS, La Salle, Universitat Ramon Llull, Barcelona, Spain (associated with ICCUB, Universitat de Barcelona, Barcelona, Spain)*

[76]*Department of Physics and Astronomy, Uppsala University, Uppsala, Sweden (associated with School of Physics and Astronomy, University of Glasgow, Glasgow, United Kingdom)*

[77]*University of Michigan, Ann Arbor, Michigan, USA (associated with Syracuse University, Syracuse, New York, USA)*

[†]Deceased.

[a]Also at Universidade de Brasília, Brasília, Brazil.

[b]Also at Central South University, Changsha, China.

[c]Also at Hangzhou Institute for Advanced Study, UCAS, Hangzhou, China.

[d]Also at Excellence Cluster ORIGINS, Munich, Germany.

[e]Also at Universidad Nacional Autónoma de Honduras, Tegucigalpa, Honduras.

[f]Also at Università di Bari, Bari, Italy.

[g]Also at Università di Bologna, Bologna, Italy.

[h]Also at Università di Cagliari, Cagliari, Italy.

[i]Also at Università di Ferrara, Ferrara, Italy.

[j]Also at Università di Firenze, Firenze, Italy.

[k]Also at Università di Genova, Genova, Italy.

[l]Also at Università degli Studi di Milano, Milano, Italy.

[m]Also at Università di Milano Bicocca, Milano, Italy.

[n]Also at Università di Padova, Padova, Italy.

[o]Also at Università di Perugia, Perugia, Italy.

[p]Also at Scuola Normale Superiore, Pisa, Italy.

[q]Also at Università di Pisa, Pisa, Italy.

[r]Also at Università della Basilicata, Potenza, Italy.

[s]Also at Università di Roma Tor Vergata, Roma, Italy.

[t]Also at Università di Siena, Siena, Italy.

[u]Also at Università di Urbino, Urbino, Italy.

[v]Also at MSU—Iligan Institute of Technology (MSU-IIT), Iligan, Philippines.

[w]Also at Universidad de Alcalá, Alcalá de Henares, Spain.